Industrial Engineering Journal
ISSN: 0970-2555
Volume : 53, Issue 9, No.2, September : 2024

RADIATION EFFECT ON MHD CONVECTIVE FLOW OF A NANOFLUID OVER AN INCLINED VERTICAL POROUS SURFACE

Dr.N.Vimala, Lecturer in Mathematics, Sri Krishnadevaraya University College of Engineering and Technology, S.K. University, Anantapur - 515 003,. A.P.,India., E-mail: vimalasku.12@gmail.com

Abstract:In the present investigation, the radiative MHD flow of an incom- pressible viscous electrically conducting non-Newtonian nanofluidover an exponentially accelerated vertical porous surface has been considered. A steady uniform magnetic field is applied under the postulation of a low magnetic Reynolds number. The ramped temperature and time-altering concentration at the surface are considered. First-order consistent chemical reaction and heat absorption are also regarded. Silver and Titania nanoparticles are disseminated in base fluid water and ethylene glycol combination should be formed by a nanofluid. The heat absorption increases the Nusselt number near the surface, while Ag and TiO2 nanoparticle volume fractions tend to lessen it. The governing non-linear partial differential equations together with boundary conditions are transformed into non-linear ordinary differential equation by using similarity transformation and are solved numerically by using versatile, extensively validated, variational finite element method. The influence of important parameters such as Lewis number (Le), buoyancy ratio parameter (Nr), Brownian motion parameter (Nb), thermophoresis parameter (Nt), radiation(An), magneticfield(M) on velocity, temperature, concentration evaluation in the boundary layer region are examined indetailed. Furthermore the effects of these parameters on local Nusselt number (Nux), local Sherwood number (Shx) and local skin friction coefficient (Cf) are also investigated. The results are compared with those are published previously and they are found in excellent agreement.
Keywords: MHD flow, Inclined Plate; Magnetic field; Radiation,FEM

1.Introduction

A nanofluid is a fluid containing small volumetric quantities of nanometer-sized particles, called nanoparticles. These fluids are envisioned to describe a fluid, in which nanometer-sized particles are suspended,in convectional heat transfer of basic fluids. The nanoparticles used in nanofluids are typically made of metals (Al, Cu), oxides (Al2O3, CuO, TiO2, SiO2), carbides (SiC), nitrides (AlN, SiN), or nonmetals (graphite, carbon nanotubes). Nanoparticles are particles with a diameter of about 1-100 nm. Nanofluids commonly contain up to a 5% volume fraction of nanoparticles to see effective heat transfer enhancements of the base fluid.To improve the thermal conductivity of these fluids nano/micro-sizedparticle materials are suspended in liquids. Several theoretical and experimental researches have been made to enhance the thermal conductivity of these fluids;Choi [1] was the first among all who introduced a new type of fluid called nanofluid while doing research on new coolants and cooling technologies. Eastman et al. [2] have noticed in an experiment that the thermal conductivity of the base fluid (water) has increased up to 60% when CuO nanoparticles of volume fraction 5% are added to the base fluid.This is because of increasing surface area of the base fluid duo to the suspension of nanoparticles. Eastman et al. [3] have also showed that the thermal conductivity has increased 40% when copper nanoparticles of volume fraction less than 1% are added to the ethylene glycol or oil. Choi et al. [4] have reported that there is 150% enhancement in thermal conductivity when carbon nanotubes are added to the ethylene glycol or oil.In addition, Xie et al. [5] have observed that Al2O3- ethylene glycol based nanofluid thermal conductivity is increased in the range 25-30% when Alumina nanoparticles are added. The enhancement in thermal conductivity of this magnitude is not only depending on the higher thermal conductivity properties of the added nanoparticles but also depending on many other mechanisms like nanoparticle size, particle agglomeration, volume fraction of the nanoparticle, Brownian motion, particle size, thermophoresis etc. We can see many research papers in literature which deals the heat and mass transfer characteristics of nanofluids by considering Brownian motion and thermophoresis effects

into account. Recently, Nield and Kuznetsov [6]have discussed the Cheng-Mincowycz problem for natural convection boundary-layer flow in a porous medium saturated nanofluid.Kuznetsov and Nield [7] studied the influence of Brownian motion and thermophoresis on natural convection boundary layer flow of a nanofluid past a vertical plate. Khan and pop [8] have discussed boundary layer flow of a nanofluid past a stretching sheet.Chamkha et al. [9]studied the mixed convectionMHD flow of a nanofluid past a stretching permeable surface in the presence of Brownian motion and thermophoresis effects.To the best of authors' knowledge, no studies have been reported in the literature to discuss MHD mixed convection heat and mass transfer characteristics of a nanofluid saturated porous medium over an inclined vertical flat plate in the presence of thermal radiation and heat generation/absorption. Hence, we made an attempt to discuss the problem here.

The recent developments in technology require an innovative revolution in heat transfer. The research on nanofluids has been amplified fast. According to reports nanofluids are advantageous heat transport fluids for engineering and manufacturing applications. The heat transport development of nanofluids is principally reliant on the heat conductivity of nanoparticles, particles' volume concentration and mass flow discharges. Under steady particles' volume concentration and flow discharges, the heat transport development only on the heat conductivity of the nanoparticles. The heat conductivity of nanoparticles may be revised or transformed by developing hybrid nanoparticles. Hybrid nanoparticles are nanoparticles created by two or additional different substantial of nanometer scale. The flu- ids developed through hybrid nanoparticles of transformed metals interested in the base fluid are recognized as hybrid nanofluids. As shown in Figure 1, with this advancement, researchers started to report several challenges associated with hybrid nanofluids soon after they came into the limelight.A large effective diversity of applications are applied in contemporary science, technol- ogy and engineering territory, such as chemical manufacture, automobile, solar collector, nuclear reactor, industrial cooling, solar synthesis, gas sensing, bio-sensing, etc. The heat transfer of effective fluids may be improved using a variety of methods. One of these is to hang nanoparticles (Cu, CuO, Ag, Fe, Au, MgO, MoS2, Al, Al2O3, TiO2, etc.) by dimension among 1 and 100 nm to the base fluid (e.g. H2O, C2H6O2 (ethylene glycol), C2nH4n+2On+1 (polyethylene-glycol), glycerine, blood, engine oil, (C6H8O6)n (sodium alginate), . . . etc.).

This to improve the constructive thermal characteristics of nanofluids and circumvent dis- crepancies in the traditional nanofluids. Sundar et al. [10] discussed that hybrid nanofluids are additional effectual heat transport fluids than solitary nanoparticle-based nanofluids or traditional fluids. Sarkar et al. [11] opined that appropriate hybridizations may create hybrid nanofluids extremely promis- ing for heat transport development; nevertheless, more investigative works are required in development and immovability, characterizations and applications to defeat the dis- putes or challenges. Devi et al. [12] explored the magnetohydrodynamic (MHD) flow of Cu-Al2O3/water hybrid nanofluids. Oxide nanoparticles have a lesser amount of heat con- ductivity than metallic nanoparticles. A superior volume fraction of oxide nanoparticles are required to have the needed heat effectiveness. The computational outcomes indicate that heat replaced the speed of Cupper-alumina/water hybrid nanofluids is more signifi- cant than that of the Cu–H2O nanofluids. The characteristics of hybrid nanofluids, based on different kinds of metallic and oxides, such as MgO, Fe3O4, Silver, copper oxide, Copper, and MWCNTs, have been demonstrated by Minea [13]. This showed most excellent viscos- ity amplification for CuO-Cu hybrid nanoparticles. Toghraie et al. [14] illustrated a variety of correlations for heat conductivities of nanofluids cleared by preceding researchers. They recommended an innovative correlation for the heat conductivity of ZnO-Titania/Ethylene Glycol hybrid nanofluids by highest accurateness using investigational findings. Hayat et al.[15] explored the three-dimensional Brinkman hybrid nanofluids models to examine the heat transport features of Copper oxide/H2O and Silver–CuO/H2O nanofluids past a lin- early stretching surface with heat radiation and homogeneous and heterogeneous reactive flows. An exhaustive and narrative review on heat transport investigation of predictable and hybrid nanofluids by the non-Newtonian fluid

model was determined by Jamshed et al.[16]and Ellahi [17]. Aman et al. [18] exhibited the sodium alginate-based hybrid nanofluids (Copper-Alumina) flow in vertical ducts. Usman et al. [19] discussed the nonlinear thermal radiation and time-dependent heat conductivity due to rotating flow alumina-H2O hybrid nanofluids past a stretching sheet with a magnetic field and buoyancy force.

The mechanical features of non-Newtonian fluids, and hear thin or shear thickness, usual stress difference, and visco-elastic reaction, may not be portrayed through the conservative theories; hence, an innovative and effectual prediction is required. Various constitutive equations portray the movement and heat transport mechanism, along with these; the Casson model has grown a great deal of acceptance. Casson fluid model becomes a non-Newtonian fluid to the investi- gators due to its wide-range applications in biomedical and industrial engineering, energy production, geophysical fluid mechanics and dynamics. Among plentiful non-Newtonian models, Casson fluid model is the mainly significant rheological model, established by Cas- son [20]. Casson fluid is a shearing thin fluid processed as one type of non-Newtonian fluid. This exhibited yield stresses. If a lesser amount of shear stress than the yield stress is applied, then the fluid performs like a solid that is, there is no flow and it moves if the applying shear stress is superior to the yield stress (Ghosh and Mukhopadhyay [21]). In this shear- ing thin fluid model, it is assumed to have an unlimited viscosity near the vanish rate of shear, yield stress below this no flow take places and a zero viscosity near an infinite rate of shear stress. Tomato sauce, Jellies, honey, human blood, soup, biological fluids, etc. are a number of frequent samples of Casson fluids. The virtual investigation of Casson fluid through homogeneous and heterogeneous reactions was examined by Khan et al. [22]. Nayak et al. [23] explored the three-dimensional unsteady MHD flow and the entropy gen- eration of micropolar Casson cross nanofluid with nonlinear thermal radiation, chemical reaction, Brownian motion, thermophoresis effect, convective boundary conditions, vis- cous dissipation and Joule heating. Rasoola et al. [24] discussed the features of Casson kind
nanofluid flow through a porous medium past a nonlinear stretching surface with heat and mass transport improvements. A numerical study of Casson nanofluid over parallel stretch- ing plane with magnetic field and Joule heating with slip and heat convective boundary conditions was presented by Kamran et al. [25].While the electromagnetic forces are discernible, the dispersal velocity of the development of ions is insignificant. As long as we believe the dispersal velocity of ions over and above such electrons, ion slips must not be overlooked. Hall and ion slip impacts come across immense solicitations specifically when reviewed in conjunction with heat transport, for instance, refrigerator convolutes, MHD vulcanization accelerators, electrical charge manufacturers, etc. Abo-Eldahab et al. [26] influenced Hall electromotive forces on the pump flow of viscous fluid through a porous medium in an unsymmetrical vertical conduit. Koumy et al. [27] scrutinized iden- tically taking Maxwell fluid toward deliberation. The performances of learning reveal that the average speed dispensation accentuates through elevated ethics of Hall parameteri- zation. Motsa and Shateyi [28] deliberated the results of Hall and ion slip for the flow of MHD micropolar fluid past the flat surface.

Industrial Engineering Journal
ISSN: 0970-2555
Volume : 53, Issue 9, No.2, September : 2024

2.Formulation of the problem

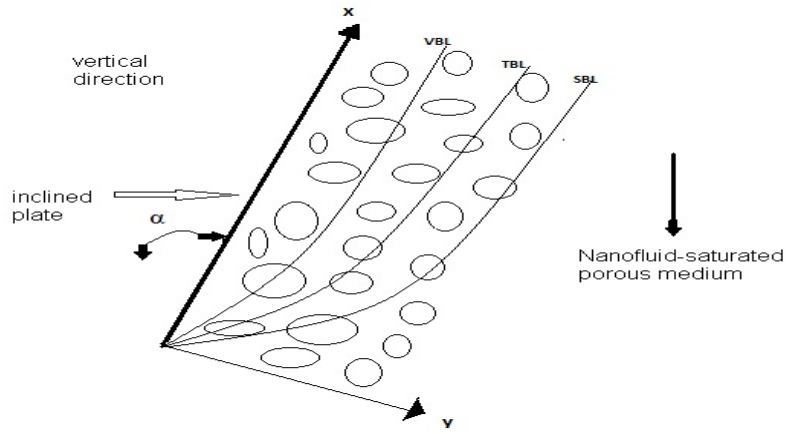

Fig.1.Configuration of the problem

Consider steady, laminar, two dimensional, incompressible, mixed convention boundary layer flow of a nanofluid along a semi-infinite inclined flat plate embedded in a nanofluid-saturated porous medium, with an acute angle α to the vertical, as depicted in Fig.1. The model used for the nanofluid incorporates the effects of Brownian motion and thermophoresis. The coordinate system is such that *x* measures the distance along the plate and *y* measures the distance normally into the fluid. The surface of plate is maintained at uniform temperature and concentration, T_w, and C_w respectively, and these values are assumed to be greater than the ambient temperature and concentration, T_∞ and C_∞, respectively. The flow is assumed to be confined in a region $y > 0$.Based on the reference works of Neild and Kuznetsov [6], by employing the Oberbeck-Boussinesq approximation and applying the boundary layer approximations, the governing equations take the following form:

$$\frac{\partial u}{\partial x}+\frac{\partial v}{\partial y}=0 \quad (1)$$

$$\frac{\partial p}{\partial y}=0 \quad (2)$$

$$\mu_f \frac{1}{\kappa}u=-\frac{\partial p}{\partial x}+g\left[(1-C_\infty)\rho_{f\infty}\beta(T-T_\infty)-(\rho_p-\rho_{f\infty})(C-C_\infty)\right]\cos\alpha-\frac{\sigma\beta_0^2}{\rho_f}u \quad (3)$$

$$\left(u\frac{\partial T}{\partial x}+v\frac{\partial T}{\partial y}\right)=\frac{k_m}{(\rho c)_f}\frac{\partial^2 T}{\partial y^2}+\frac{(\rho c)_p}{(\rho c)_f}\left[D_B\frac{\partial C}{\partial y}.\frac{\partial T}{\partial y}+\left(\frac{D_T}{T_\infty}\right)\left(\frac{\partial T}{\partial y}\right)^2\right]-Q(T-T_\infty)-\frac{1}{(\rho c)_f}.\frac{\partial}{\partial y}(q_r) \quad (4)$$

$$\frac{1}{\varepsilon}\left(u\frac{\partial C}{\partial x}+v\frac{\partial C}{\partial y}\right)=D_B\frac{\partial^2 C}{\partial y^2}+\left(\frac{D_T}{T_\infty}\right)\frac{\partial^2 T}{\partial y^2} \quad (5)$$

The boundary conditions based on the problem description are as follows:

$$u=0,\quad T=T_w,\quad C=C_w \text{ at } y=0 \quad (6)$$

$$u=u_\infty,\quad T\longrightarrow T_\infty,\quad C\longrightarrow C_\infty \text{ at } y=\infty \quad (7)$$

p may be eliminated from Eqs. (2) and (3) by cross-differentiation and the continuity equation (1) will be satisfied introducing a stream function ψ defined by the Cauchy-Riemann equations:

$$u=\frac{\partial \psi}{\partial y},\qquad v=-\frac{\partial \psi}{\partial x} \quad (8)$$

By substituting Eqn (8) in Eqs (3), (4), (5), we arrive at the following three coupled similarity equations:

$$\frac{\partial^2\psi}{\partial y^2}=\left[\frac{(1-c_\infty)\rho_{f\infty}\beta g k}{\mu}\frac{\partial T}{\partial y}-\frac{(\rho_p-\rho_{f\infty})gk}{\mu}\frac{\partial c}{\partial y}\right]\cos(\alpha)-\frac{\sigma\beta_0^2}{\rho}u \quad (9)$$

$$\frac{\partial\psi}{\partial y}\frac{\partial T}{\partial x}-\frac{\partial\psi}{\partial x}\frac{\partial T}{\partial y}=\frac{k_m}{(\rho c)_f}\frac{\partial^2 T}{\partial y^2}+\frac{\varepsilon(\rho c)_p}{(\rho c)_f}\left[D_B\frac{\partial c}{\partial y}\frac{\partial T}{\partial y}+\left(\frac{D_T}{T_\infty}\right)\left(\frac{\partial T}{\partial y}\right)^2\right]-Q(T-T_\infty)-\frac{1}{(\rho c)_m}\frac{\partial}{\partial y}(q_r) \quad (10)$$

$$\frac{1}{\varepsilon}\left(\frac{\partial\psi}{\partial y}\frac{\partial c}{\partial x}-\frac{\partial\psi}{\partial x}.\frac{\partial c}{\partial y}\right)=D_B\frac{\partial^2 C}{\partial y^2}+\left(\frac{D_T}{T_\infty}\right)\frac{\partial^2 T}{\partial y^2} \quad (11)$$

The following similarity transformations are introduced to simplify the mathematical analysis of the problem

Industrial Engineering Journal
ISSN: 0970-2555
Volume : 53, Issue 9, No.2, September : 2024

$$\eta = \frac{y}{x} Pe_x^{1/2}, \qquad f(\eta) = \frac{\psi}{\alpha_m Pe_x^{1/2}}, \qquad \theta(n) = \frac{T-T_\infty}{T_w-T_\infty}, \qquad \phi(n) = \frac{C-C_\infty}{C_w-C_\infty} \tag{12}$$

where, $\alpha_m = \frac{k_m}{(\rho c)_f}$.

By using Rosseland approximation for radiation, the radiative heat flux q_r is defined as

$$q_r = -\frac{4\sigma^*}{3K^*}\frac{\partial T^4}{\partial y}, \tag{13}$$

whereσ^* is the Stephan-Boltzman constant, K^* is the mean absorption coefficient. We assume that the temperature differences within the flow are such that the term T^4 may be expressed as a linear function of temperature. This is accomplished by expanding T^4 in a Taylor series about a free stream temperature T_∞ as follows:

$$T^4 = T_\infty{}^4 + 4T_\infty{}^3(T-T_\infty) + 6T_\infty{}^2(T-T_\infty)^2 + \cdots \tag{14}$$

Neglecting higher-order terms in the above Eq. (19) beyond the first degree in$(T-T_\infty)$, we get

$$T^4 \cong 4T_\infty{}^3 T - 3T_\infty{}^4 . \tag{15}$$

Thus substituting Eq. (20) in Eq. (18), we get

$$q_r = -\frac{16T_\infty{}^3\sigma^*}{3K^*}\frac{\partial T}{\partial y}. \tag{16}$$

Using equations (12) and (16), the governing non-linear partial differential equations (9) - (11) together with boundary conditions (6) and (7) reduce to

Momentum boundary layer equation:

$$f'' = \frac{Ra_x}{Pe_x}(\theta' - Nr\,\varphi')Cos(\alpha) + Mf' \tag{17}$$

Thermal boundary layer equation:

$$\left(1+\frac{4}{3}An\right)\theta'' + \frac{1}{2}f\,\theta' + Nb\,\theta'\varphi' + Nt(\theta')^2 - Q\theta = 0 \tag{18}$$

Concentration (species diffusion) boundary layer equations:

$$\varphi'' + \frac{1}{2}Le\,\varphi' + \frac{Nt}{Nb}\theta'' = 0 \tag{19}$$

The transformed boundary conditions are

$$\eta = 0, \quad f = 0, \quad \theta = 1, \quad \phi = 1.\eta \longrightarrow \infty, \quad f' = 1, \quad \theta = 0, \quad \phi = 0. \tag{20}$$

wherea prime denotes differentiation with respect to η, and the key thermophysical parameters dictating the flow dynamics are defined by

$$Nr = \frac{(\rho_p - \rho_{f\infty})(C_w - C_\infty)}{\rho_{f\infty}\beta(T_w - T_\infty)(1-C_\infty)}, \qquad Nb = \frac{\varepsilon\beta(\rho c)_p D_B(C_w - C_\infty)}{(\rho c)_f\ \alpha_m}, Nt = \frac{\varepsilon(\rho c)_p D_T(T_w - T_\infty)}{(\rho c)_f\ \alpha_m T_\infty}$$

$$Le = \frac{\alpha_m}{\varepsilon D_B}, \quad Ra_x = \frac{(1-C_\infty)Kg\beta\rho_{f\infty}(T_w - T_\infty)x}{\mu\alpha_m}, \quad Pe_x = \frac{U_\infty x}{\alpha_m},$$

$$Ra = \frac{Ra_x}{Pe_x}, \qquad Q = \frac{x^2}{Pe_x\alpha_m}, \qquad An = \frac{4T_\infty{}^3\sigma^*}{K^*\alpha_m}, \qquad M = \frac{\sigma\beta_0^2 x}{\rho P e_x^{1/2}}.$$

Where Le, Nr, Nb,Nt,Ra_x, Pe_x, M, Q and An are Lewis number, buoyancy ratio parameter, Brownian motion parameter, thermophoresis parameter, local Darcy-Rayleigh number, local Peclet number, magnetic field parameter, heat generation/absorption parameter and thermal radiation parameterrespectively. We note that porosity (ε) is absorbed into the Nb, Nt and Le parameters, and therefore it is not explicitly simulated in this study.Quantities of practical interest in this problem are the local Nusselt number Nu_x, and the local Sherwood number Sh_x, are defined as

$$Nu_x = \frac{xq_w}{k(T_w - T_\infty)} Sh_x = \frac{xq_m}{D_B(C_w - C_\infty)} \tag{21}$$

Here, q_w, q_m are the heat flux and mass flux at the surface (plate), respectively. Using (17) we obtain dimensionless versions of these key design quantities:

$$(Pe_x)^{-1/2}Nu_x = -\theta'(0), \quad (Pe_x)^{-1/2}Sh_x = -\phi'(0), \tag{22}$$

Industrial Engineering Journal
ISSN: 0970-2555
Volume : 53, Issue 9, No.2, September : 2024

In the present context, $(Pe_x)^{-1/2}Nu_x$ *and* $(Pe_x)^{-1/2}Sh_x$ are referred to as the reduced Nusselt number and reduced Sherwood numbers which are represented by $-\theta'(0)$ *and* $-\phi'(0)$ respectively. The set of ordinary differential equations (17) – (19)are highly non-linear, and therefore cannot be solved analytically. The finite-element method has been implemented to solve these non-linear equations. The very important aspect in this numerical procedure is to select an approximate finite value of η_∞. So, in order to estimatethe relevant value of η_∞, the solution process has been started with an initial value of $\eta_\infty = 4$, and then the equations (17) – (19) are solved together with boundary conditions (20). We have updated the value of η_∞ and the solution process is continued until the results are not affected with further values of η_∞.The choice of $\eta_{max} = 8$ *and* $\eta_{max} = 5$for temperature and concentration have confirmed that all the numerical solutions approach to the asymptotic values at the free stream conditions.

3.Analysis of the numerical results

Nanofluids are prepared using single-step and two-step techniques. The first one is predominantly used to produce hybrid nanofluids on a small scale. The second one is suitable for mass production. It is considered an unsteady MHD Darcy flow of an incompressible viscous elec- trically conducting non-Newtonian Casson hybrid nanofluid over an infinite, exponentially accelerated vertical surface under the influence of slip velocity in a rotating frame taking Hall and ion slip impacts into account. Water and ethylene glycol mixture has been taken as a base nano fluid. The exact solutions of the governing equations of the flow domain are obtained using the Laplace transform method. The flow is presided over by the non- dimensional parameters.Comprehensive numerical computations were conducted for different values of the parameters that describe the flow characteristics, and the results are illustrated graphically and in tabular form. Selected graphical profiles are presented in Figs. 2-9.

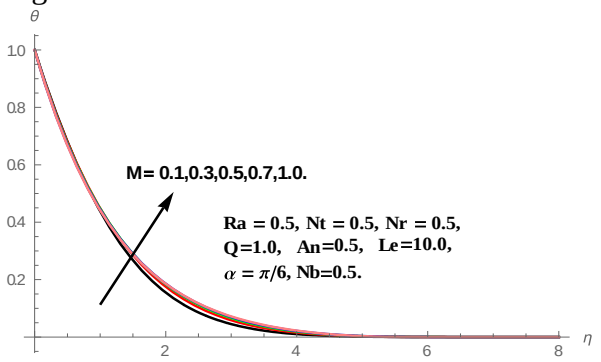

Fig.2. Temperature profiles for different values of M.

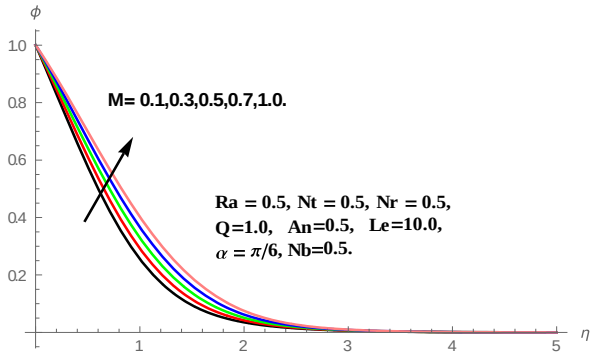

Fig.3. Concentration profiles for various values of M.

The influence of magnetic field parameter (M) on temperature and concentration profiles in the boundary layer is depicted in Fig.2 - 3. It is noticed from these figures that the thermal boundary layer thickness as well as the solutal boundary layer thickness enhances with enhance in the values of

M. This is because of the fact that, the presence of magnetic field in an electrically conducting fluid produces a force called Lorentz force, this force acts against the flow direction causes the depreciation in velocity profiles, and at the same time, to overcome the drag force imposed by the Lorentzian retardation the fluid has to perform extra work; this supplementary work can be converted into thermal energy which increases the temperature of the fluid (Fig.2), this force also increases the concentration profiles(Fig.3).

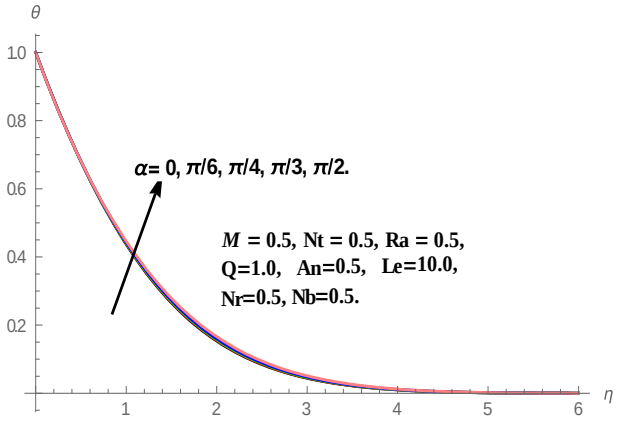

Fig.4. Temperature profiles for different values of α.

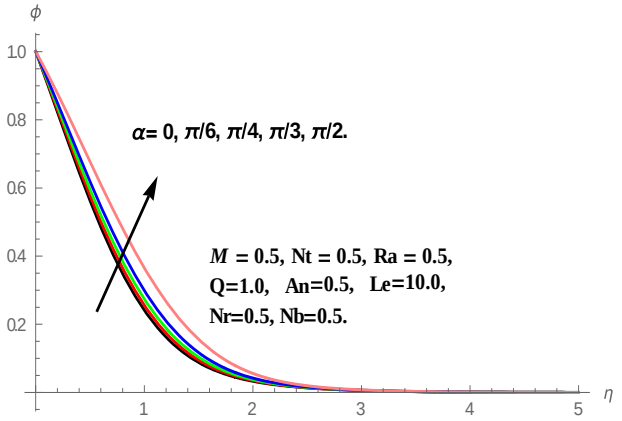

Fig.5. Concentration profiles for different values of α.

The variation in temperature and concentration profiles for different values of plate inclination angle (α) is depicted in Fig.4 and 5. It is noticed from fig.4 that,anincrease in plate inclination angle(α) resist the motion of the fluid and is causes an enhancement in the temperature of the fluid (Fig.4). It is also observed that the concentration distributions are increased with increase in the values of α (Fig.5). This elevation in temperature and concentration profiles is because of the reduction inbuoyancy ratio term in the momentum equation with increasing values of α. It is also noticed that the maximum buoyancy force occur for α =0 for the same temperature and concentration differences (vertical plate) and there is no buoyancy term when α =π/2 (horizontal plate), as the above term vanishes. From these two figures we conclude that both thermal boundary layer and solutal boundary layers elevates with the plate inclination angle α.

Industrial Engineering Journal
ISSN: 0970-2555
Volume : 53, Issue 9, No.2, September : 2024

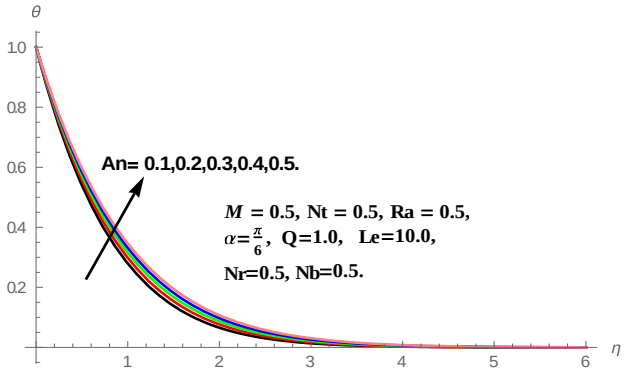

Fig.6. Temperature profiles for various values of An.

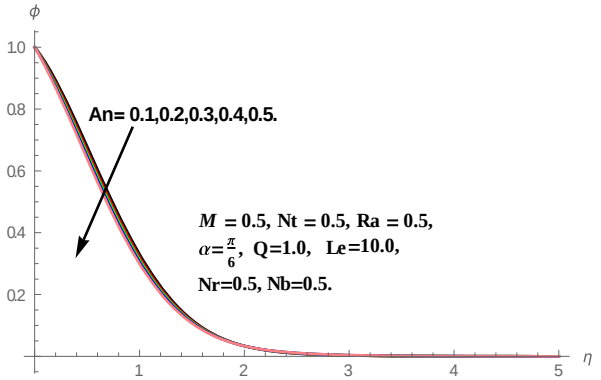

Fig.7.Concentration profiles for various values of An

The effect of Brownian motion parameter Nb on temperature and concentration profiles is illustrated in fig.6 and 7. It is noticed that, with the increasing values of Brownian motion parameter Nb temperature profiles enhanced as shown in Fig.6, whereas concentration profiles depreciates with enhancing values of Nb (Fig.7). This type of tendency in temperature and concentration is same as in the case of general heat transfer fluids. Many theoretical studies suggested that, enhancement in thermal conduction of the fluid by Brownian motion of nanoparticles is because of any one of the following two mechanisms; either a direct effect owing to nanoparticles that transport heat or an indirect contribution due to micro-convection of fluid surrounding individual nanoparticles. Clearly, we noticed that Brownian motion parameter has significant enhancing influence on both temperature and concentration profiles.

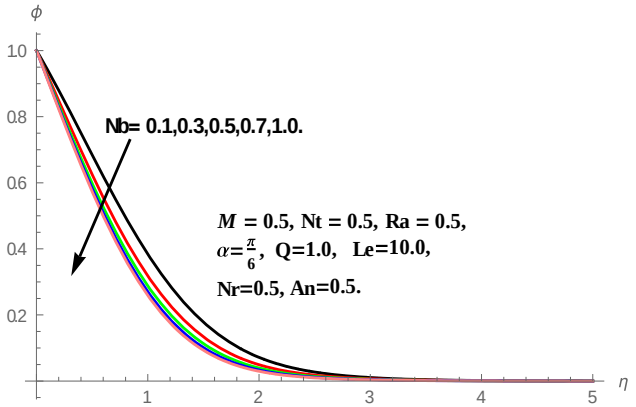

Fig..8 .Concentration profiles for various values of Nt.

Industrial Engineering Journal
ISSN: 0970-2555
Volume : 53, Issue 9, No.2, September : 2024

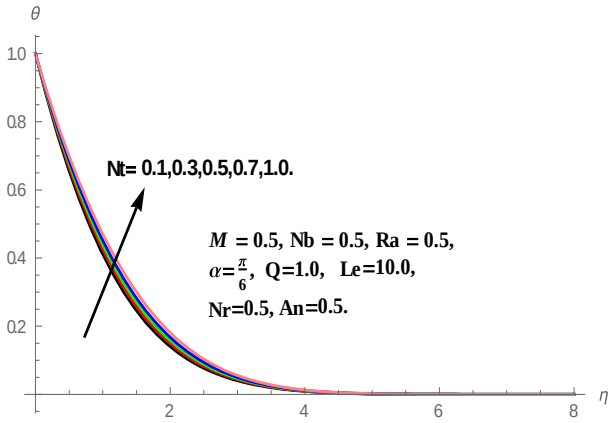

Fig..9 . Temperature profiles for various values of Nt.

Variation of non-dimensional temperature and concentration distributions for different values of thermophoretic parameter Nt is depicted in Fig.8 and 9. It is noticed from these figures that both temperature and concentration profiles elevates in the boundary layer region for thehigher values of thermophoretic parameter Nt. This is from the reality that particles near the hot surface create thermophoretic force; this force enhances the temperature and concentration of the fluid in the fluid region. We noticed from Fig. 8 that the temperature differences are small, this is because of the fact that thermophoretic parameter is a nanoscale parameter so that its influence is relatively less.

Table.1. Variation of Nur and Shr with Pr, Nb and Nr for Nt= 0.1, Nc = 10 and Le = 10.

N_b	N_r	P_r=1		P_r=5		P_r=10	
		Nu	Sh	Nu	Sh	Nu	Sh
0.1	0.1	0.4616	0.9578	0.4023	1.1682	0.2386	1.3022
	0.2	0.4584	0.9447	0.3989	1.1551	0.235	1.2892
	0.3	0.4551	0.9309	0.3952	1.1414	0.2313	1.2756
	0.4	0.4517	0.9164	0.3915	1.1271	0.2275	1.2613
	0.5	0.4481	0.9012	0.3875	1.1121	0.2235	1.2464
	0.6	0.4442	0.885	0.3834	1.0962	0.2193	1.2307
	0.7	0.4402	0.8677	0.379	1.0794	0.2149	1.2141
	0.8	0.4189	1.0185	0.3556	1.2301	0.1907	1.3645
0.3	0.1	0.4168	1.0067	0.3532	1.2185	0.1883	1.3531
	0.2	0.4146	0.9945	0.3508	1.2066	0.1858	1.3412
	0.3	0.4122	0.9817	0.3482	1.1941	0.1832	1.3289
	0.4	0.4098	0.9684	0.3456	1.1811	0.1805	1.3161
	0.5	0.4073	0.9544	0.3429	1.1676	0.1778	1.3027
	0.6	0.4047	0.9397	0.34	1.1534	0.1749	1.2887
	0.7	0.4019	0.9241	0.337	1.1385	0.1719	1.274
	0.8	0.378	1.0334	0.3105	1.2463	0.1444	1.3812
0.5	0.1	0.3763	1.0221	0.3086	1.2352	0.1425	1.3702
	0.2	0.3745	1.0103	0.3066	1.2237	0.1405	1.3588
	0.3	0.3727	0.998	0.3046	1.2118	0.1385	1.347
	0.4	0.3708	0.9852	0.3025	1.1994	0.1364	1.3348
	0.5	0.3688	0.9717	0.3004	1.1864	0.1342	1.322
	0.6	0.3668	0.9577	0.2981	1.1729	0.1319	1.3087
	0.7	0.3646	0.9428	0.2958	1.1588	0.1296	1.2948
	0.8	0.125	-0.025	0.025	0.12	-0.15	0.235

The data in Table .1 indicate how the reduced Nusselt and Sherwood numbers are affected by the changes in the Prandtl number Pr, the Brownian motion parameter Nb and the buoyancy parameter

Nb when the rest of the parameters are fixed at the valuesindicated in the table heading. For every combination of Nb and Nr, both the reduced Nusselt and reduced Sherwood numbers increase with the increase in Pr. For a fixed Pr, both the reduced Nusselt number and the reduced Sherwood number decrease as Nb and Nr each increase. Table .2 allows the reader to see how the changes in the Lewis affect the reduced Nusselt number and the reduced Sherwood number. As the Lewis number increases the reduced Nusselt number increases slightly but there is a substantial increase in the reduced Sherwood number. Tables.1 and 2 provide infor- mation about the heat and mass transfer characteristics of the flow in a form convenient for research and engineering calculations.

Table.2. Variation of Nu and Sh with Le, Nb and Nr for Nt =0.1, Nc =10 and Pr=10.

N_b	N_r	Le = 1		Le = 5		Le = 10	
		Nu	Sh	Nu	Sh	Nu	Sh
0.1	0.1	0.4896	1.1204	0.3932	1.1728	0.492	1.3097
	0.2	0.4866	1.1078	0.3898	1.1602	0.4886	1.2972
	0.3	0.4834	1.0947	0.3864	1.1471	0.485	1.2842
	0.4	0.4801	1.0809	0.3827	1.1334	0.4813	1.2706
	0.5	0.4767	1.0664	0.379	1.1191	0.4775	1.2563
	0.6	0.4731	1.0512	0.375	1.1041	0.4735	1.2414
	0.7	0.4692	1.035	0.3709	1.0882	0.4693	1.2257
	0.8	0.4652	1.0177	0.3665	1.0714	0.4649	1.2091
0.3	0.1	0.4439	1.1685	0.3431	1.2221	0.4407	1.3595
	0.2	0.4418	1.1567	0.3407	1.2105	0.4383	1.3481
	0.3	0.4396	1.1445	0.3383	1.1986	0.4358	1.3362
	0.4	0.4372	1.1317	0.3357	1.1861	0.4332	1.3239
	0.5	0.4348	1.1184	0.3331	1.1731	0.4305	1.3111
	0.6	0.4323	1.1044	0.3304	1.1596	0.4278	1.2977
	0.7	0.4297	1.0897	0.3275	1.1454	0.4249	1.2837
	0.8	0.4269	1.0741	0.3245	1.1305	0.4219	1.269
0.5	0.1	0.403	1.1834	0.298	1.2383	0.3944	1.3762
	0.2	0.4013	1.1721	0.2961	1.2272	0.3925	1.3652
	0.3	0.3995	1.1603	0.2941	1.2157	0.3905	1.3538
	0.4	0.3977	1.148	0.2921	1.2038	0.3885	1.342
	0.5	0.3958	1.1352	0.29	1.1914	0.3864	1.3298
	0.6	0.3938	1.1217	0.2879	1.1784	0.3842	1.317
	0.7	0.3918	1.1077	0.2856	1.1649	0.3819	1.3037
	0.8	0.3896	1.0928	0.2833	1.1508	0.3796	1.2898

4.References:

[1] Choi S.U.S,Enhancing thermal conductivity of fluids with nanoparticles, developments and applications of non-Newtonian flows, in: D.A. Siginer, H.P. Wang (Eds.), FED—Vol. 231/MD, Vol. 66, The American Society of Mechanical Engineers, New York, pp. 99–105,(1995).

[2] Eastman. J.A, Choi. S.U.S, Li.S, Thompson.L.J.andLee.S, Enhanced thermal conductivity through the development of nanofluids, in: S. Komarneni, J.C. Parker, H.J. Wollenberger (Eds.), Nanophase and Nanocomposite Materials II, MRS, Pittsburg, PA, pp.3–11, (1997).

[3] Eastman. J.A, Choi. S.U.S, Li.S, Yu. W andThompsonL.J, Anomalously increased effective thermal conductivities of ethylene glycol-based nano-fluids containing copper nano-particles, Appl. Phys. Lett. 78, 718–720, (2001).

[4] Choi. S.U.S, Zhang.Z.G, Yu.W, Lockwood.F.E and Grulke. E.A, Anomalous thermal conductivity enhancement in nano-tube suspensions, Appl. Phys. Lett. 79 , 2252–2254, (2001).

[5] Xie. H, Wang.J, Xi.T, Liu.Y, Ai.F and Wu.Q, Thermal conductivity enhancement of suspensions containing nanosized alumina particles, J. Appl. Phys. 91, 4568–4572, (2002).
[6] Nield.D.A, and Kuznetsov.A.V, The Cheng-Minkowycz problem for natural convection boundary-layer flow in a porous medium saturated by a nanofluid,Int. J. Heat Mass Transfer 52,5792–5795, (2009).
[7] Kuznetsov.A.V. andNield. D.A, Natural convection boundary-layer of a nanofluid past a vertical plate, Int. J. Therm. Sci. 49, 243–247, (2010).
[8]Khan. W. A, and Pop. I, Boundary-layer flow of a nanofluid past a stretching sheet, Int. J. Heat Mass Transfer 53, 2477–2483, (2010).
[9] Chamkha. A.J, Aly.A.M andAl-Mudhaf.H, Laminar MHD mixed convection flow of a nanofluid along a stretching permeable surface in the presence of heat generation or absorption effects, Int. J. Microscale Nanoscale Thermal Fluid Transp. Phenom 2, Article 3, (2011).
[10] Sundar LS, Sharma KV, Singh MK, et al. Hybrid nanofluids preparation, thermal properties, heat transfer and friction factor – a review. Renew Sustain Energy Rev. 2017;68:185–198. doi:10.1016/j.rser.2016.09.108.
[11] Sarkar J, Ghosh P, Adil A. A review on hybrid nanofluids: recent research, development and applications. Renew Sustain Energy Rev. 2015;43:164–177. doi:10.1016/j.rser.2014.11.023.
[12] Devi SPA, Devi SSU. Numerical investigation of hydromagnetic hybrid Cu-Al2O3/water nanofluid flow over a permeable stretching sheet with suction. Int J Nonlin Sci Num Simul. 2016;17:249–257. doi:10.1515/ijnsns-2016-0037.
[13] Minea AA. Challenges in hybrid nanofluids behavior in turbulent flow: recent research and numerical comparison. Renew Sustain Energy Rev. 2017;71:426–434.
[14] Toghraie D, Vahid AC, Masoud A. Measurement of thermal conductivity of ZnO–TiO2/EG hybrid nanofluid. J Thermal Anal Cal. 2016;125:527–535.
[15] Hayat T, Nadeem S. Heat transfer enhancement with Ag–CuO/water hybrid nanofluid. Results Phys 2017;7:2317–2324.
[16] Jamshed W, Aziz A. A comparative entropy based analysis of Cu and Fe3O4/methanol Powell-Eyering nanofluid in solar thermal collectors subjected to thermal radiation, vari- able thermal conductivity and impact of different nanoparticles shape. Results Phys. 2018;9: 195–205.
[17] Ellahi R. Special issue on recent developments of nanofluids. Appl Sci. 2018;8:192.
[18] Aman S, Zokri SM, Ismail Z, et al. Effect of MHD and porosity on exact solutions and flow of a hybrid Casson-nanofluid. J Adv Res Fluid Mech Therm Sci. 2018;44:131–139.
[19] Usman M, Hamid M, Zubair T, et al. Cu-Al2O3/water hybrid nanofluid through a permeable sur- face in the presence of nonlinear radiation and variable thermal conductivity via LSM. Int J Heat Mass Transf. 2018;126:1347–1356.
[20] Casson N. A flow equation for pigment oil suspensions of the printing ink type. Oxford: Pergamon Press; 1959.
[21] Ghosh S, Mukhopadhyay S. MHD slip flow and heat transfer of Casson nanofluid over an exponentially stretching permeable sheet. Int J Auto Mech Eng. 2017;14(4):4785–4804.
[22] Khan MI, Waqas M, Hayat T, et al. A comparative study of Casson fluid with homogeneous-heterogeneous reactions. J Colloid Interface Sci. 2017;498:85–90. doi:10.1016/j.jcis.2017.03. 024.
[23] Nayak MK, Hakeem AKA, Ganga B, et al. Entropy optimized MHD 3D nanomaterial of non-Newtonian fluid: a combined approach to good absorber of solar energy and intensification of heat transport. Comput Methods Programs Biomed. 2020;186:105131. doi:10.1016/j.cmpb.2019. 105222.
[24] Rasoola G, Chamkha AJ, Muhammad T, et al. Darcy-Forchheimer relation in Casson type MHD nanofluid flow over non-linear stretching surface. Propulsion Power Res. 2020;9(2):159–168. doi:10.1016/j.jppr.2020.04.003.
[25] Kamran A, Hussain S, Sagheer M, et al. A numerical study of magnetohydrodynamics flow in Casson nanofluid combined with Joule heating and slip boundary conditions. Results Phys. 2017;7:3037–3048. doi:10.1016/j.rinp.2017.08.004.

[26] Abo-Eldahab E, Barakat E, Nowar K. Hall currents and heat transfer effects on peristaltic transport in a vertical asymmetric channel through a porous medium. Math Prob Eng. 2012;2012:840203. doi:10.1155/2012/840203.
[27] Koumy SRE, Barakat ESI, Abdelsalam SI. Hall and porous boundaries effects on peristaltic trans- port through porous medium of a Maxwell model. Transp Porous Media. 2012;94:643–658.
[28] Motsa SS, Shateyi S. The effects of chemical reaction, Hall and ion-slip currents on MHD micropo- lar fluid flow with thermal diffusivity using a novel numerical technique. J Appl Math. 2012: 1–30. doi:10.1155/2012/689015.
[29] Asghar S, Hussain Q, Hayat T, et al. Hall and ion slip effects on peristaltic flow and heat transfer analysis with Ohmic heating. Appl Math Mech. 2014;35:1509–1524.
[30] Krishna MV, Chamkha AJ. Hall and ion slip effects on MHD rotating boundary layer flow of nanofluid past an infinite vertical plate embedded in a porous medium. Results Phys. 2019;15:102652. doi:10.1016/j.rinp.2019.102652.
[31] Krishna MV, Swarnalathamma BV, Chamkha AJ, et al. Joule and Hall effects on MHD rotating mixed convective flow past an infinite vertical porous plate. J Ocean Eng Sci. 2019;4(3):263–275. doi:10.1016/j.joes.2019.05.002.
[32] Krishna MV, Chamkha AJ. Hall and ion slip effects on unsteady MHD convective rotating flow of nanofluids – application in biomedical engineering. J Egyptian Math Soc. 2020;28(1):1–14. doi:10.1186/s42787-019-0065-2.
[33] Krishna MV. Heat transport on steady MHD flow of copper and alumina nanofluids past a stretching porous surface. Heat Transfer. 2020;49:1374–1385. doi:10.1002/htj.21667.
[34] Krishna MV, Ahamad NA, Chamkha AJ. Hall and ion slip effects on unsteady MHD free convec- tive rotating flow through a saturated porous medium over an exponential accelerated plate. Alexandria Eng J. 2020;59:565–577. doi:10.1016/j.aej.2020.01.043.
[35] Krishna MV, Sravanthi CS, Gorla RSR. Hall and ion slip effects on MHD rotating flow of ciliary propulsion of microscopic organism through porous media. Int Commun Heat Mass Transfer. 2020;112:104500. doi:10.1016/j.icheatmasstransfer.2020.104500.
[36] Krishna MV, Chamkha AJ. Hall and ion slip effects on MHD rotating flow of elastico-viscous fluid through porous medium. Int Commun Heat Mass Transfer. 2020;113:104494. doi:10.1016/j.icheatmasstransfer.2020.104494.